Progress In Electromagnetics Research Letters, Vol. 77, 123–128, 2018

A Balanced Bandpass Filter with Ultra-Wide Stopband and Common-mode Suppression

Zhi-Jie Yang[1], Yang-Yang Shan[1], Xin-Tong Zou[1], Feng Wei[1, *], and Bin Li[2]

Abstract—A balanced-to-balanced (BTB) bandpass filter (BPF) with an ultra-wide upper stopband is proposed in this letter. The proposed BPF is fed by balanced stepped-impedance microstrip-to-slotline transition structures. Good differential-mode (DM) transmission and common-mode (CM) suppression can be achieved intrinsically. To achieve good quality in DM passband and out-of-band suppression, a pair of dual-mode resonators has been designed and adopted. Meanwhile, the proposed balanced BPF exhibits an ultra-wide upper stopband of 162.7%. In order to verify the feasibility of the design method, a balanced BPF with a centre frequency of 1.57 GHz has been fabricated and measured. Measured results indicate that the designed filter achieves an out-of-band rejection better than 15 dB from 1.85 to 18 GHz, and the insertion loss (IL) inside the passband less than 1.4 dB. A good agreement between the simulation and measurement results demonstrates the validity of the design.

1. INTRODUCTION

In recent years, balanced/differential circuits have attracted substantial attentions due to their excellent performances in terms of the immunity of environmental noises and interferences, compared with the single-end counterparts. Bandpass filters (BPFs) are essential devices in the RF front end of wireless communication systems, and their performance in the field of selectivity and out-of-band suppression has attracted increasingly attentions. Several balanced BPFs with good common-mode (CM) suppression were presented in [1–3]. Along with the usage of transmission lines, spurious passbands become inevitable on account of periodic behavior in frequency. Presence of undesired spurious bands or harmonics would seriously degrade the performance and application of microwave and millimeter wave circuits. Therefore, many methods have been devoted to stopband extension. In [4], the realization of planar wideband bandpass filters with an extremely wide upper stopband was described. A compact wideband bandpass filter with a very wide stopband for terrestrial radio (TETRA) band applications was proposed in [5]. Four periodical tapered structures were adopted in [6] to obtain a wide stopband response, which increases the filter size and insertion loss. In [7], a novel quad-mode resonator composed of a stepped-impedance ring resonator (SIRR) with two pairs of shorted stubs was proposed to design a dual-band BPF, which achieves a wide upper stopband. What's more, a novel balanced wide-stopband single-band BPF with high selectivity and CM suppression was presented in [8]. A novel wideband balanced filter with wide stopband using asymmetrical coupled lines and stubs was presented in [9], which can be realized a wideband CM suppression. Stepped coupled lines were used to replace the coupled lines to extend the upper stopband.

In this letter, a balanced BPF with an ultra-wide upper stopband is designed and fabricated. The designed filter is fed by balanced stepped-impedance microstrip-to-slotline transition structures, which

Received 25 June 2018, Accepted 26 July 2018, Scheduled 1 August 2018

* Corresponding author: Feng Wei (fwei@mail.xidian.edu.cn).

[1] Collaborative Innovation Center of Information Sensing and Understanding at Xidian University and Science and Technology on Antenna and Microwave Laboratory, Xidian University, Xi'an 710071, P. R. China. [2] School of Information and Electronics, Beijing Institute of Technology Beijing, P. R. China.

enables the proposed filter to achieve independent CM responses with a larger bandwidth and a higher suppression. Furthermore, the designed dual-mode resonator can achieve harmonic suppression and weaken the influence of spurious signals. The predicted results on S-parameters have been compared with the measured ones, and a reasonable agreement is achieved.

2. THEORETICAL ANALYSIS

The proposed balanced ultra-wide stopband BPF is realized by integrating the proposed dual-mode resonators with the balanced stepped-impedance microstrip-to-slotline transition structures, which is symmetric with respect to O-O' plane, as shown in Fig. 1. The black blocks stand for the microstrip lines on the top surface of the substrate, and the gray blocks represent the slotline on the bottom surface. Each transition structure comprises a U-type stepped-impedance microstrip feedline and a stepped-impedance slotline resonator. The U-type microstrip line is coupled with the slotline by means of the magnetic field. Because of the geometrical symmetry, the balanced circuit can be analyzed using the DM and CM method. The cross-views of electrical field distribution at T-T' plane indicated in the Fig. 1 are shown in Fig. 2, which are herein used for demonstrating its working mechanism. When a DM excitation is applied, a virtual electrical wall can be obtained at plane O-O'. A quasi transverse electromagnetic slotline mode generates a virtual electrical wall at the same plane, as illustrated in Fig. 2(a). Through strong magnetic coupling, the DM signals along the U-type microstrip line can be converted successfully into the slotline mode propagating along the slotline and be transferred to the next transition. Therefore, good DM transmission can be realized. Under CM operation, a virtual magnetic wall at O-O' plane is formed, as shown in Fig. 2(b). Due to the magnetic wall perpendicular to the electric field of the slotline mode, which conflicts with the magnetic wall's boundary condition, the CM signals are blocked and a better CM suppression is achieved. In the end, balanced microstrip-to-slotline transition structures are employed to transformation between the slotline modes and the microstrip line modes. The slotline can be viewed as a transmission line when truncated along the center. Furthermore,

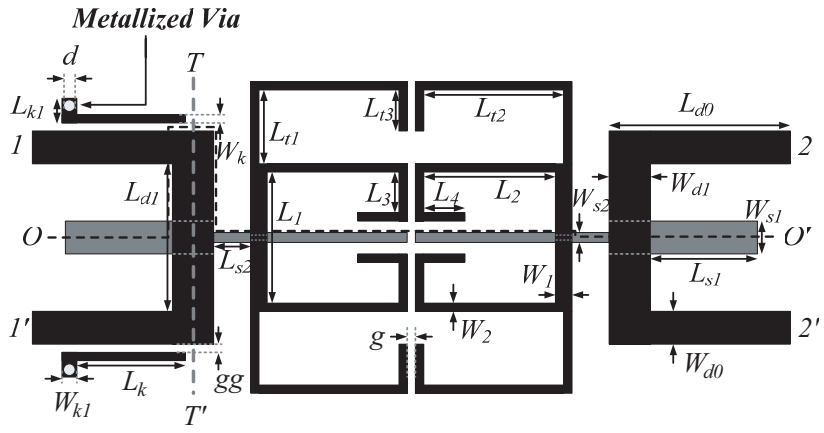

Figure 1. Configuration of the proposed balanced BPF.

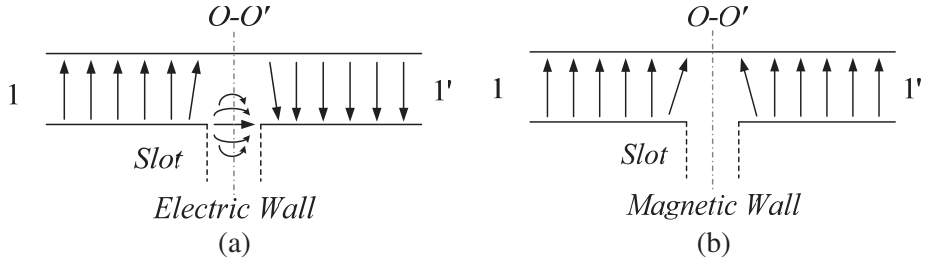

Figure 2. The cross-views of electrical field distribution at T-T' plane. (a) Under DM operation. (b) Under CM operation.

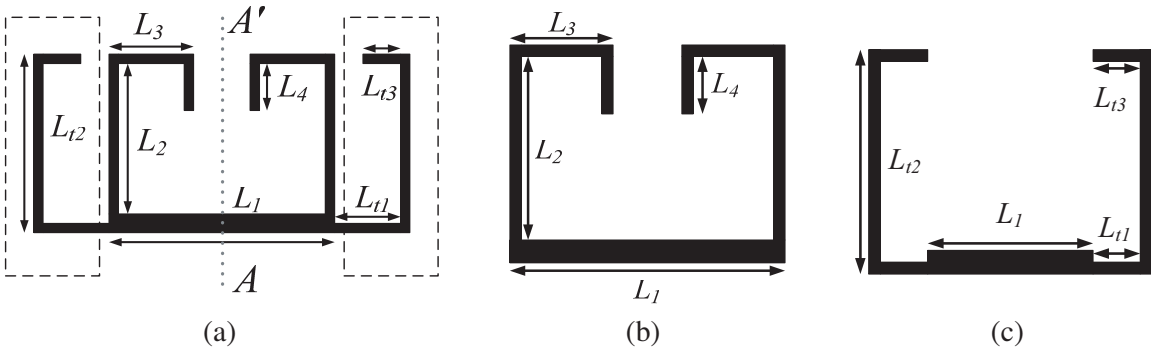

Figure 3. The structure of resonator. (a) The proposed dual-mode resonator, (b) resonator I, and (c) resonator II.

the key of this work turns to focus on the design of the DM passband and stopband extension.

Figure 3(a) shows the structure of the proposed dual-mode resonator, which is symmetrical to the A-A' plane. The proposed resonator can be realized by integrating a half-wavelength stepped-impedance resonator (SIR) with two open-stubs, which are denoted with the dotted boxes. Furthermore, the proposed dual-mode resonator can be viewed as two different SIRs, which were represented as resonator I and II respectively, as shown in Figs. 3(b) and (c).

Conveniently, the SIRs can be simply viewed approximately as two different uniform impedance resonators (UIRs). Therefore, the resonant frequencies of SIRs can be expressed as about equations:

$$f_1 \approx \frac{c}{4(L_1 + L_2 + L_3 + L_4)\sqrt{\varepsilon_{eff}}} \tag{1}$$

$$f_2 \approx \frac{c}{4(L_1 + L_{t1} + L_{t2} + L_{t3})\sqrt{\varepsilon_{eff}}} \tag{2}$$

It can be shown that the resonator frequencies are directly related to the lengths of high-impedance stubs. When adjusting the lengths of L_4 and L_{t3}, the resonator frequencies f_1 and f_2 will change correspondingly. The simulation results of the effects of the dimensions on the DM resonant frequencies are analyzed and shown in Fig. 4. The simulation results confirm the correctness of the theoretical analysis.

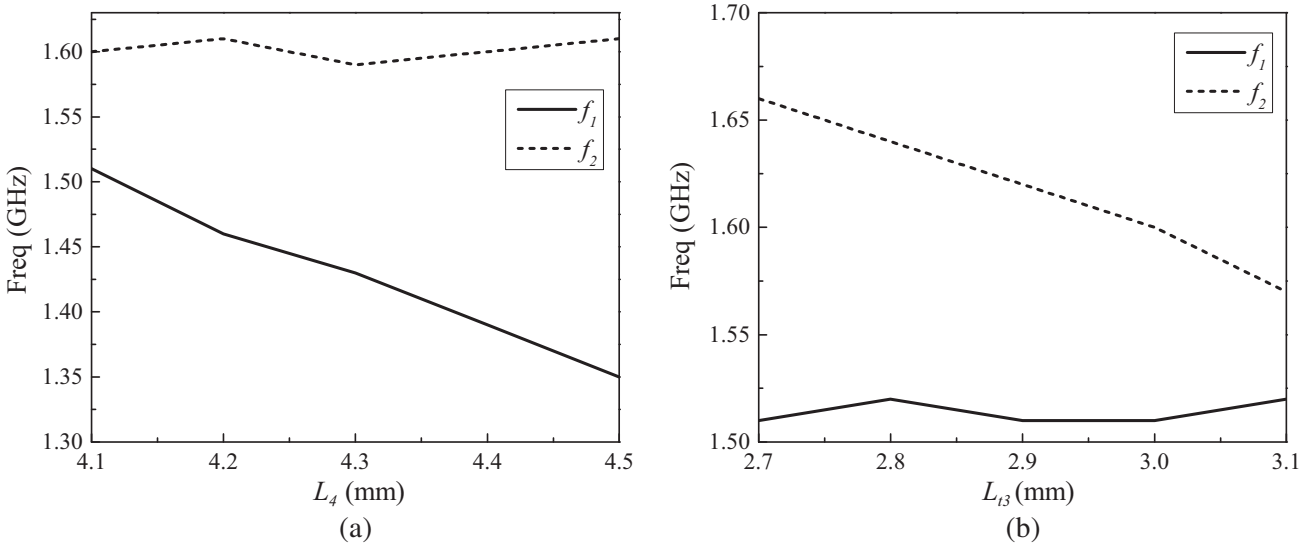

Figure 4. The simulated DM resonant frequencies of the BPF with different dimensions. (a) L_4. (b) L_{t3}.

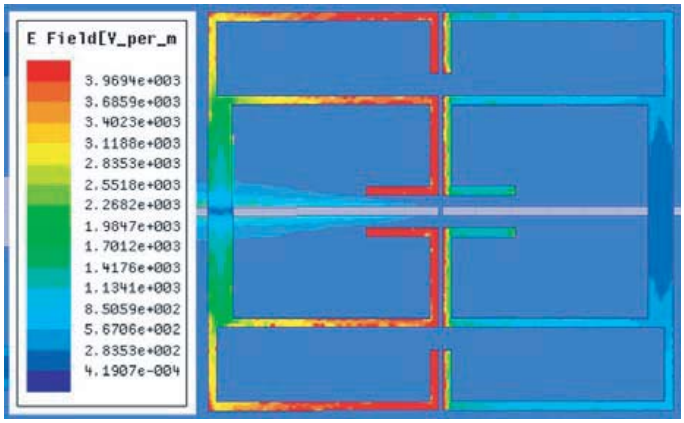

Figure 5. The electric field pattern of the proposed dual-mode resonator.

On the other hand, the resonant frequencies of the proposed resonator are directly related to the impedance ratios and the electrical lengths of two transmission lines. By adjusting these parameters properly, the parasitic resonant frequencies can be kept away from the fundamental resonant frequencies. When two fundamental resonant frequencies f_1 and f_2 are close enough, a DM passband with good out-of-band rejection will appear. What's more, a pair of quarter wavelength resonators has been added in both sides of the balanced input port *1-1'* to terminate the fifth harmonic. The electric field pattern of the proposed dual-mode resonator simulated by HFSS is shown in Fig. 5. Therefore, an ultra-wide upper stopband with a satisfying suppression is realized by these methods mentioned above.

3. SIMULATED AND MEASURED RESULTS

The S-parameters of the proposed filter were measured with an Agilent VNA (vector network analyzer) N5222. The effective dimension of the fabricated filter is only $62.2\,mm \times 25.1\,mm$ ($0.31\lambda_g \times 0.13\lambda_g$, where λ_g is the guide wavelength at 1.5 GHz). All the dimensions of the proposed balanced filter are selected as follows: $W_{d0} = 2.45$ mm, $W_{d1} = 3.2$ mm, $W_{s1} = 4.0$ mm, $W_{s2} = 0.5$ mm, $W_1 = 1.4$ mm, $W_2 = 0.5$ mm, $W_k = 0.5$ mm, $W_{k1} = 1.0$ mm, $L_{d0} = 15$ mm, $L_{d1} = 15.2$ mm, $L_{s1} = 6.8$ mm, $L_{s2} = 3.0$ mm, $L_1 = 12.0$ mm, $L_2 = 11.1$ mm, $L_3 = 4.6$ mm, $L_4 = 3.6$ mm, $L_{t1} = 4.2$ mm, $L_{t2} = 12.0$ mm, $L_{t3} = 2.95$ mm, $L_k = 6.4$ mm, $L_{k1} = 2$ mm, $g = 0.1$ mm, $gg = 0.5$ mm, $d = 0.8$ mm. The characteristics of the DM and CM frequency responses of the balanced BPF mentioned above are simulated and analyzed by EM simulation software HFSS 13.0. The adopted substrate is F4BM-2 with a thickness of 0.8 mm and a dielectric constant of 2.2.

Figure 6 compares the simulated DM and CM responses with the measured ones among 0.5–3 GHz. The measured minimum insertion loss is 1.4 dB and maximum reflection loss is better than 15.5 dB within the passband. Meanwhile, the measured CM suppressions are greater than 50 dB around the DM passband. In addition, one transmission zero (TZ) on the left side of the passband at 1.38 GHz reinforced the selectivity. It is expected that the deviations of the measured results and the simulated ones are caused by the reflections from the SMA connectors and the finite substrate.

As shown in Fig. 7, the DM spurious frequency bands of the balanced filter are suppressed to greater than 15 dB, and the upper stopband can be extended to 18 GHz, that is, eleven times the centre frequency of the proposed filter. The upper stopband covers 1.85–18 GHz and the relative bandwidth is about 162.7%. The measured data have a good agreement with the simulated responses. Fig. 8 shows the photographs of the fabricated balanced BPF with ultra-wide stopband.

A comparison with some previously reported wide stopband BPFs is available in Table 1. Compared with the published works listed in Table 1, the proposed balanced BPF has great advantage in the immunity of environmental noises and interferences and stopband bandwidth, which achieves a high CM suppression of 60 dB and an out-of-band suppression of 15 dB. Meanwhile, the insertion loss of the proposed balanced BPF is better than the works presented in [7–9]. To sum up, the proposed balanced filter has a good competitiveness in the future practical applications.

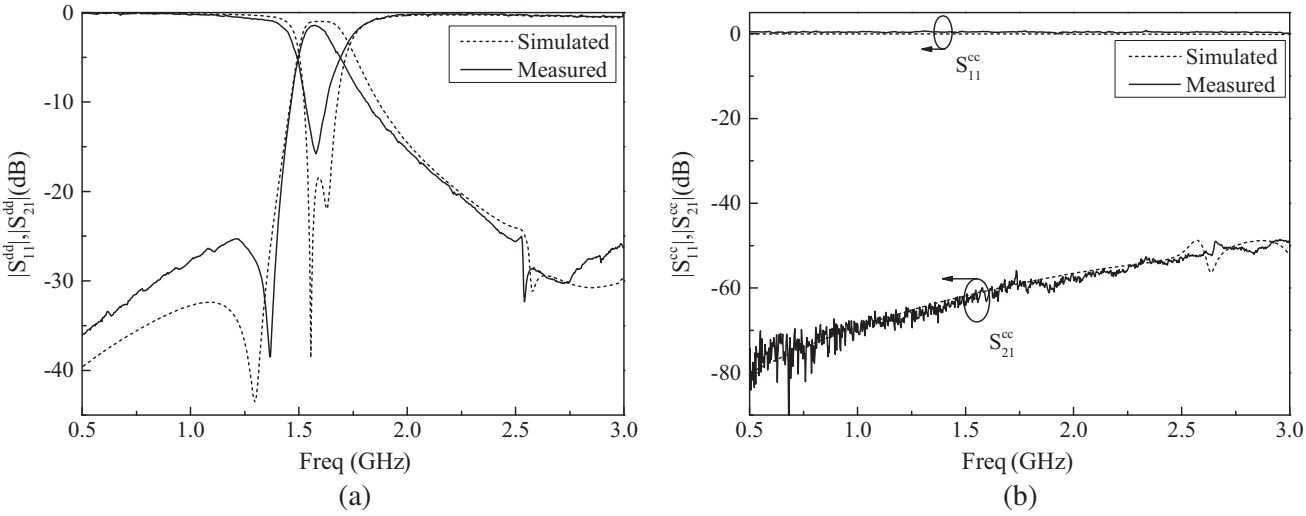

Figure 6. Comparisons of the simulated and measured results (Narrowband view). (a) DM reflection loss and insertion loss and (b) CM reflection loss and insertion loss.

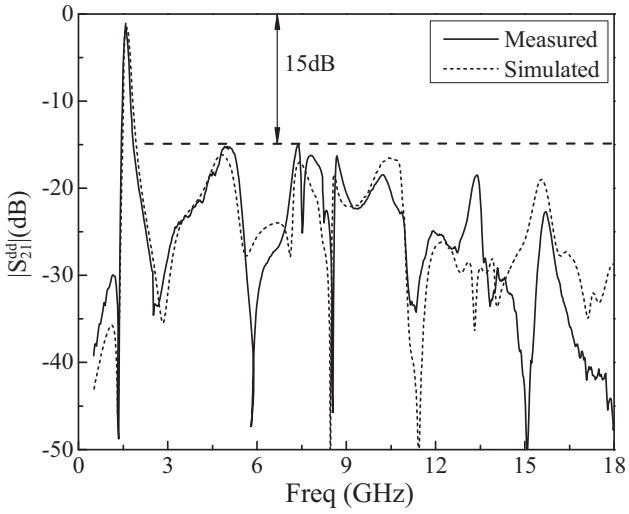

Figure 7. Comparison of the simulated and measured results (Wideband view).

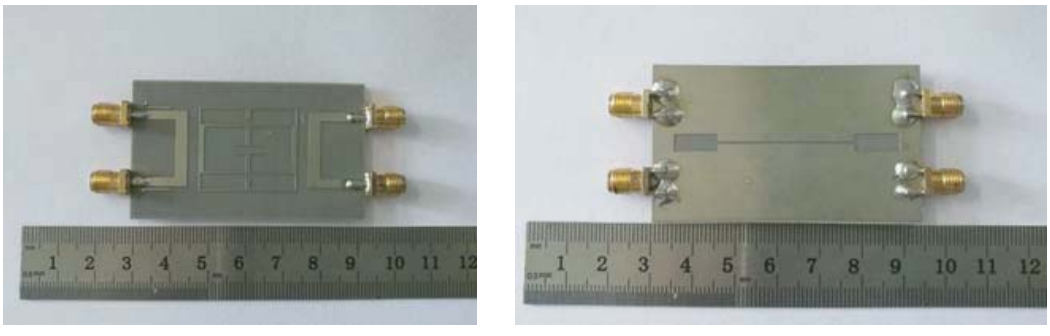

Figure 8. Photographs of the fabricated balanced BPF with ultra-wide stopband. (a) Top layer and (b) bottom layer.

Table 1. Comparison with some reported wide stopband BPFs.

	Type	IL (dB)	CM suppression (dB)	Effective size (λ_g^2)	Stopband relative bandwidth (%)
Ref. [6]	Unbalanced	1.0	none	0.5×0.1	152.5
Ref. [7]	Unbalanced	2.48/3.6	none	Unknown	84.2
Ref. [8]	Balanced	2.0	40	0.13×0.19	153.9
Ref. [9]	Balanced	2.2	11	0.3×0.37	81.3
Our work	Balanced	1.4	60	0.31×0.13	162.7

4. CONCLUSION

In this letter, a balanced ultra-wide upper stopband BPF has been proposed and analyzed. The building blocks of the filter are a pair of dual-mode resonators and the microstrip-to-slotline transmission structures. Using this topology, a balanced BPF with a centre frequency of 1.57 GHz has been designed, fabricated and measured. The CM suppression of the proposed balanced BPF shows a good character. Significantly, the proposed BPF boasts an ultra-wide upper stopband up to 18 GHz, and is expected to suppress the spurious eleventh harmonic. Ultra-wide stopband bandwidth of the filter makes it strong in rejecting unwanted interfering and noise signals. The measured results are in a good agreement with the simulated ones showing that the filter is viable for usage in practical environment.

ACKNOWLEDGMENT

This work was supported by the Basic Research Foundation of Beijing Institute of Technology (grant 20170542009) and the Fundamental Research Funds for the Central Universities (grant JB180204).

REFERENCES

1. Shi, J. and Q. Xue, "Balanced bandpass filters using center-loaded half-wavelength resonators," *IEEE Trans. Microw. Theory Techn.*, Vol. 58, 970–977, 2010.
2. Qiang, J., J. Shi, and Q. Cao, "Compact differential wideband bandpass filters based on half-wavelength lines," *IEEE Microw. Wirel. Compon. Lett.*, Vol. 27, 906–908, 2017.
3. Shi, J., C. Shao, and J.-X. Chen, "Compact low-loss wideband differential bandpass filter with high common-mode suppression," *IEEE Microw. Wirel. Compon. Lett.*, Vol. 23, 480–482, 2013.
4. Malherbe, J. A. G., "Wideband bandpass filter with extremely wide upper stopband," *IEEE Trans. Microw. Theory Techn.*, Vol. 66, 2822–2827, 2018.
5. Killamsetty, V. K. and B. Mukherjee, "Miniaturised highly selective bandpass filter with very wide stopband using meander coupled lines," *Electron. Lett.*, Vol. 53, 889–890, 2017.
6. Li, L., Z. F. Li, and Q. F. Wei, "Compact and selective lowpass filter with very wide stopband using tapered compact microstrip resonant cells," *Electron. Lett.*, Vol. 45, 267–268, 2009.
7. Shi, J., L. L. Lin, J.-X. Chen, H. Chu, and X. Wu, "Dual-band bandpass filter with wide stopband using one stepped-impedance ring resonator with shorted stubs," *IEEE Microw. Wirel. Compon. Lett.*, Vol. 24, 442–444, 2014.
8. Shi, J. and Q. Xue, "Dual-band and wide-stopband single-band balanced bandpass filters with high selectivity and common-mode suppression," *IEEE Trans. Microw. Theory Techn.*, Vol. 58, 2204–2212, 2010.
9. Ma, X., W. Feng, H. Chen, and W. Yang, "Balanced filter with wide stopband using asymmetrical coupled lines," *IEEE 2017 Asia Microwave Conference*, 638–640, 2017.